DOppo

in Climatic Processes & Climate Sensitivity, Geophys. Monogr. Ser 29 eds. J.E Hansen + T. Takahashi 48-57 Am Geophys. Un. Washington DC, 1984

VARIATION OF MONSOONAL UPWELLING: A RESPONSE TO CHANGING SOLAR RADIATION

Warren L. Prell

Department of Geological Sciences, Brown University, Providence, RI 02912-1846

Abstract. In the western Arabian Sea, the distribution of planktonic foraminifera is related to coastal upwelling and therefore to the low-level summer monsoon winds which force the upwelling. Records of faunal variation over the past 30 kyr reveal that the Indian Ocean summer monsoon has been both stronger (9 kyr) and weaker (18 kyr). These paleoceanographic reconstructions and analogies to general circulation model simulations suggest that changes in the distribution of seasonal solar radiation and surface albedo are responsible for the changes in monsoon intensity. This study illustrates that the Milankovitch Hypothesis of climate change, which changes the seasonal distribution of solar radiation as a function of orbital variations, applies to low-latitude as well as high-latitude climate changes.

Introduction

Paleoceanographic records can be used to infer the relative importance of various climate processes in the past. However, such inferences must be based on a clear strategy that relates climatic processes with paleoceanographic data. First, one must select a part of the climate system that has a well-known forcing that causes a specific and strong oceanic response. Next, the oceanic response must have a geologic record that can be calibrated to modern environmental conditions. If these criteria can be met, then a time series of the paleoceanic index may be used to interpret the relative importance of past climatic processes.

The Indian Ocean summer monsoon is a distinct climatic phenomenon associated with a specific upwelling response that, in turn, is recorded in deep-sea sediments. This geologic time series of monsoonal upwelling can be used to address the following questions. How has the Indian Ocean summer monsoon behaved over the past 30,000 years? What climatic mechanisms and processes are consistent with past variations of the monsoon? Do changes in seasonal solar radiation affect low-latitude climate, and in particular, monsoonal upwelling.

To answer these questions, I have studies the spatial and temporal distribution of planktic for aminifers in the Arabian Sea. The patterns of faunal variation have been related to patterns of sea surface temperature and coastal upwelling and therefore to the windfield. These data and modern relationships are used to reconstruct the relative intensity of the Indian Ocean monsoon over the past 30 kyr. This study concentrates on the changing direction and intensity of low-level winds and their effect on coastal upwelling in the western Arabian sea.

Models for the Intensity of Indian Ocean Monsoon Circulation Patterns

The Indian Ocean summer monsoon is a global phenomenon as well as an intense seasonal variation of climate on the regional scale. The characteristics and causes of the Indian Monsoon circulation have been the subject of numerous books (for example, Ramage, 1971; Miller and Keshavamurthy, 1968), papers, and intensive large-scale studies (Garp, 1981). The synoptic patterns and atmospheric dynamics of the Southwest Indian Monsoon are extremely complex and only their large-scale time-averaged characteristics will be examined here.

Past variations in the strength of the Southwest Monsoon may be interpreted to reflect changes in large-scale boundary conditions of the climate. Figure 1 illustrates the major components of the Southwest Monsoon in conceptual fashion. In this simplified view of the Southwest Monsoon, the major boundary conditions are the Indian Ocean SST, the size and elevation of the Asian continent, the surface albedo of the Asian continent, and the seasonal distribution of solar radiation. The major response to these boundary conditions is the near-surface heating of Asia during the summer. This summer heating, which is due to the low heat capacity of the continent, creates the low pressure zone over Asia relative to the Indian Ocean, which has relatively constant SST and sea-level atmospheric pressure. This pressure gradient between the Asian continent

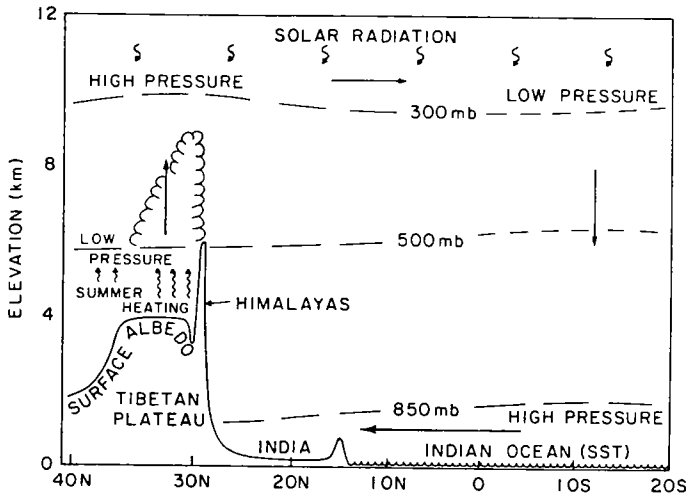

Fig. 1. Conceptional illustration of the boundary conditions and climate processes controlling the Southwest Indian Monsoon circulation. The elevations of isobar surfaces are somewhat exaggerated to show the gradients.

and the Indian Ocean reverses seasonally and is the primary cause of the low level Southwest Monsoon winds.

The relative importance of these various boundary conditions can be inferred from synoptic studies and general circulation model (GCM) experiments. In particular, GCM results have provided insight into the importance of topography, albedo, and solar radiation on the intensity of the Southwest Monsoon. Hahn and Manabe (1975) used the GFDL GCM to show that the great elevation of the Tibetan Plateau in central Asia was responsible, in part, for the great intensity of the Southwest Monsoon. Simulations with no mountains gave a much weaker monsoonal circulation. Hence, the topography of the Tibetan Plateau in central Asia is thought to be an important boundary condition for the Southwest Monsoon. This continental elevation is considered constant over 10^3 years but may not be constant over intervals of 10^5 to 10^6 years.

The effect of surface albedo over Asia on the monsoon was demonstrated by Manabe and Hahn (1977). Their simulation of the last glacial maximum produced a weaker monsoonal circulation, which they attributed to the effect to higher albedo over Asia. An experiment using modern terrestrial boundary conditions and glacial SSTs (CLIMAP, 1976) generated a monsoon circulation with an intensity similar to modern conditions. Hence, Manabe and Hahn concluded that albedo changes were more important than SST changes in controlling the intensity of the monsoonal circulation. Importantly, the solar radiation during the summer at 18,000 YBP is very similar to modern conditions.

Recent experiments by Kutzbach (1981) and Kutzbach and Otto-Belisner (1982) have demonstrated the importance of changes in seasonal radiation patterns. They simulated the climate at 9,000 YBP by utilizing modern boundary conditions and imposing the solar radiation pattern of 9,000 YBP. Their results showed an intensified monsoonal circulation, with low level winds over the Arabian Sea increased by almost 50%. This set of simulations clearly indicates that simple changes in the distribution of seasonal solar radiation can cause major fluctuations of the Southwest Monsoon. In light of these observations and our simple model of the monsoon

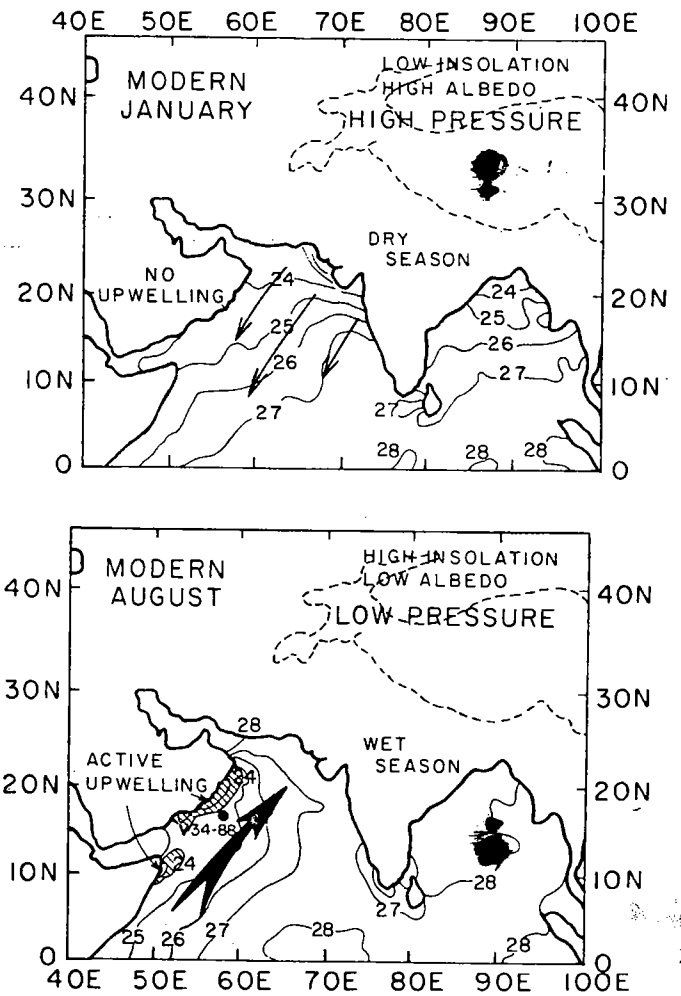

Fig. 2. Top: Boundary conditions and circulation for the modern winter monsoon. The dashed line over Asia indicates elevations greater than 3000 meters. The shaded area shows the distribution of SSTs less than 27°C. The circulation arrows indicate moderate wind speeds. Bottom: Boundary conditions and circulation during the modern summer monsoon. Cold water (shaded area is less than 27°C) is concentrated along the western Arabian Sea and the upwelling (diagonal lines show SSts less than 24°C) is active off arabia. The bold arrow represents high wind speeds and intense circulation.

/igure 1), the geologic data will be nterpreted in terms of changes in Indian Ocean SST, surface albedo, and solar radiation.

Atmospheric Circulation of the Modern Monsoon

The near-surface winds of the Arabian Sea are characterized by a complete reversal on a seasonal basis. The winter Northeast Monsoon is characterized by low seasonal insolation over Asia and relatively high albedo due to seasonal snow cover. These boundary conditions produce a high pressure cell in the low-level atmosphere over Asia which results in a northeasterly wind flow over the Arabian Sea (Figure 2a). During the winter monsoon (December, January, and February), winds are from the northeast off Asia with relatively low velocities.

The summer Southwest Monsoon is characterized by high seasonal insolation over Asia and relatively low albedo (Figure 2b). These conditions create a low-level, low-pressure cell centered at about 30°N over Asia. During this season, the southern Indian Ocean acts as a high pressure cell and the resulting wind flow is from the southwest across the Arabian Sea (see Figure 2b). During the summer monsoon (June, July, and August), the winds are from the southwest at extremely high velocities. Long-term climate records (sixty years) show that the resultant winds over much of the western Arabian Sea average >10 ms^{-1} during this season (Hastenrath and Lamb, 1979). This dramatic reversal and increased intensity of the winds is also associated with major changes in cloudiness, heat transport, and precipitation.

Oceanic Circulation of the Modern Monsoon

The response of the Arabian Sea to the atmospheric forcing is most clearly observed in the sea-surface temperature (SST) patterns. During the winter monsoon, the isotherms of the Arabian Sea are roughly trend from east-west to northeast-southwest with lower SSTs (23°C) to the north and higher SSTs (27°C) to the south (Figure 2a, Hastenrath and Lamb, 1979). Much of the Arabian Sea and Bay of Bengal are less than 27°C due to lowered insolation and northerly wind flow. The cool waters off Africa represent southward transport in the winter Somali Current.

This relatively simple pattern completely changes during the summer monsoon when the isotherms trend roughly northeast-southwest parallel to the coasts of Africa and Arabia (Figure 2b). During the summer, a time of expected high temperatures at this latitude, long-term average SSTs as low as 22°C to 23°C are observed along the coast of Africa and Arabia and grade to 27°C to 28°C in the central Arabian Sea (Hastenrath and Lamb, 1979). The reason for this abrupt change in the SST pattern is the coastal upwelling along the coast of

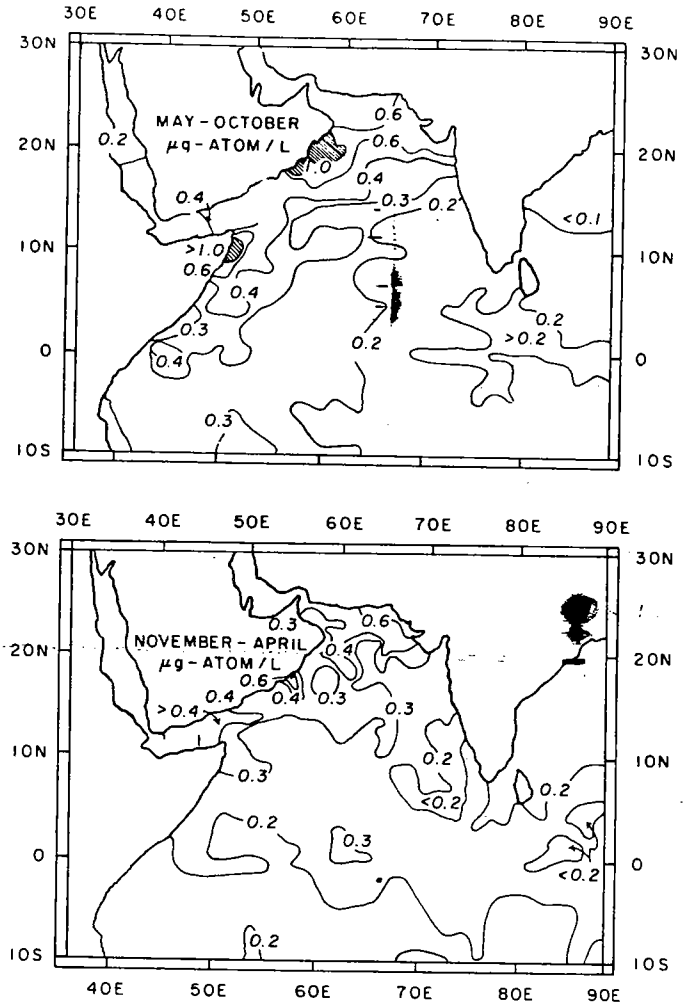

Fig. 3. Phosphorus content of the surface waters (g-atom per liter) for the summer half-year (May to October) and the winter half-year (November to April). Redrawn from Wyrtki, 1971.

Africa and Arabia. This upwelling brings cooler waters to the surface and distorts the normal seasonal pattern (Duing and Leetma, 1980; Prell and Streeter, 1982). During the Southwest Monsoon interval, about 66% of the variance in local SST anomalies along the coast of Arabia can be explained by simple Ekman transport (Prell and Streeter, 1982). Hence, the monsoonal winds and coastal SST are closely linked during the summer.

The effect of coastal upwelling is also observed in various chemical and biotic measures. For example, the concentration of nutrients (Wyrtki, 1971) and chlorophyll (Krey and Babenerd, 1976) in the surface waters show intermediate values during the winter half-year whereas they show high values along the coast of Africa and Arabia during the summer half-year (Figure 3). These nutrient concentrations negatively covary with the SST to provide a geographic pattern for the variation of coastal

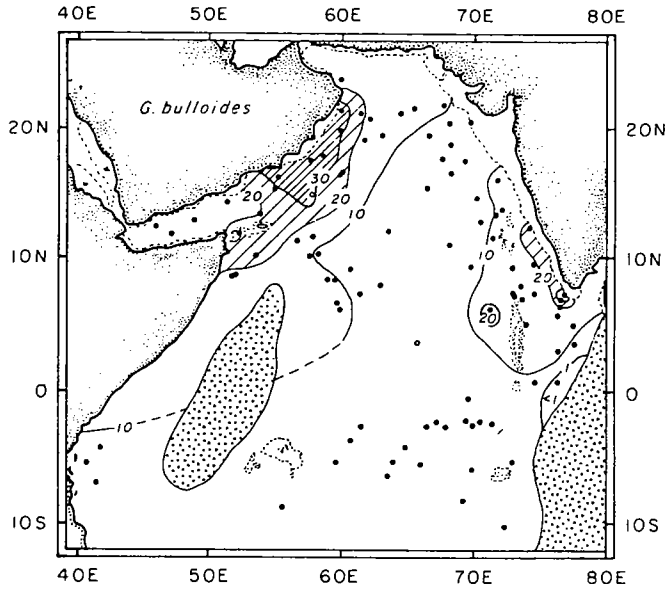

Fig. 4. The percent of G. bulloides in surface sediments of the Arabian Sea. Note that G. bulloides maximum abundance coincides with low SST (Figure 2b) and high nutrient content (Figure 3) of the surface waters. Samples in the dotted areas contain less than 10 forams/g and have not been used to construct species biogeography.

upwelling and its associated effects. These data show that monsoonal upwelling is a strong and spatially restricted oceanographic response that can be used as a measure of monsoonal wind intensity.

Plankton Patterns

The plankton of the Indian Ocean, specifically the planktic foraminifers, respond to the SST and chemical gradients caused by monsoonal upwelling. Eventually, the foraminifers are deposited in the underlying sediments to preserve a record of changes in monsoonal upwelling. The response of the planktic foraminifers can be determined by mapping their distribution in the surficial sea-floor sediments and comparing their abundance and size gradients to various upwelling-associated gradients such as SST.

Among the various planktic foraminifers in the Indian Ocean, one species in particular, Globigerina bulloides, seems particularly well attuned to the environments caused by upwelling. A map of the relative abundance of G. bulloides reveals that it is most abundant along the coast of Arabia and decreases in abundance toward the central Arabian Sea (Figure 4). The abundance of G. bulloides off southwest India is associated with another upwelling system (i.e. lower SSTs), which is probably remotely forced. This spatial pattern is similar to that of the summer SST (Figure 2b) and phosphate content (Figure 3). A lack of suitable samples prevents us from documenting a similar pattern off the coast of Somalia. The relative abundance of G. bulloides versus the sea-surface temperatures during August, a measure of the upwelling gradient, gives a correlation coefficient of -0.91 (Figure 5). Although some scatter exists in this core-top data set, the high degree of correlation clearly documents that G. bulloides is associated with the monsoonal upwelling pattern.

I have used the abundance of a single species, G. bulloides rather than the somewhat standard factor analysis assemblages and SST estimates for several reasons. First, in the Northern Indian Ocean, the major factor assemblage associated with upwelling contains significant abundances of both G. bulloides and Globigerinita glutinata (Cullen, 1980). G. bulloides is clearly associated with low-latitude upwelling zones, such as off North Africa (Ganssen and Sarnthein, 1983) and in the Cariaco Trench, Caribbean Sea (Rogl and Bolli, 1973 and references therein). However, no clear association with environmental data or upwelling exist for the species G. glutinata. Second, the calibration of paleotemperature equations for the Northern Indian Ocean is complex and in need of further study. In ocean-wide equations such as FI-2 (Hutson and Prell, 1980), G. bulloides is a sub-polar species and is associated with SSTs much less than in the Arabian Sea upwelling zone. Preliminary attempts at local calibrations (Cullen, 1980) have produced noisy estimates with low multiple correlation

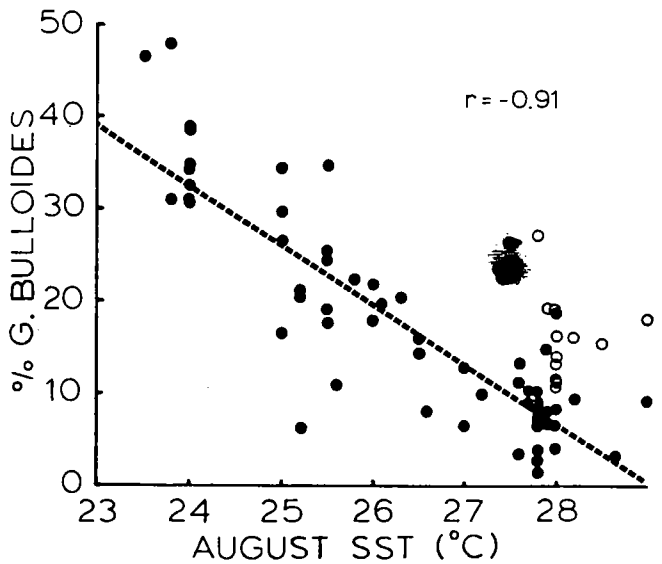

Fig. 5. The abundance of G. bulloides in the surface sediments versus August SST (°C). Filled circles represent open Arabian Sea samples and open circles represent Chargos-Lacadive Sea samples. The correlation of SST and G. bulloides in open Arabian Sea samples is -0.91.

coefficients for the Southwest Monsoon season. In addition, the definition of seasonality is complicated in the Arabian Sea. In light of these possible sources of misinterpretation, I have elected to use a single species index, which is imperfect, but at this time probably the best index of upwelling.

A subset of samples also reveals that the average size of G. bulloides increases with cooler temperatures or toward the upwelling maxima. Hence, G. bulloides is largest where it is most abundant, another indication that the upwelling zone is its optimum environment. These abundance data relate the distributon of planktic foraminifers in the deep-sea sediments to the environmental patterns of monsoonal upwelling, and in turn, to the intensity of monsoonal winds. Hence, the abundance of G. bulloides will be used as an indication of the intensity of monsoonal upwelling. Next, we examine the geologic record of this index of monsoonal upwelling.

Records of Monsoonal Upwelling

The relative abundance of G. bulloides has been measured in the late Quaternary sections of nine Arabian Sea cores (Figure 6). The two transects of cores represent conditions proximal to the coastal upwelling zone (A-A′) and conditions in the eastern Arabian Sea and the central Arabian Sea (B-B′) distal to the upwelling. Examination of the abundance data and the oxygen isotope stratigraphy in each core (Figure 6) reveals several distinct patterns.

The oxygen isotope stratigraphy reveals that all records extend from the late Holocene at core-top through Termination I (isotope stage 1/2 boundary), include isotope stage 2 (the last glacial maximum), and most extend into isotope stage 3. Termination I is characterized by a rapid $\delta^{18}O$ depletion and has little secondary structure in the low accumulation rate cores but displays more structure in cores with high accumulation rates. Core MD77-203 exhibits a two-stage termination (1a and 1b) similar to that observed in the Atlantic Ocean (Duplessy et al., 1981). Here, we are interested in the G. bulloides abundance relative to the isotope stratigraphy.

The first major faunal pattern is that G. bulloides decreases in abundance away from the coast (Figure 6). Maximum values range from over 40% near the coast (MD77-203 and RC9-161) to less than about 10% in the eastern and central Arabian Sea (for example, V34-101 and V19-188). This gradient persists throughout the 30,000-year record but is significantly lower during certain intervals.

A second major pattern is the relative abundance peak of G. bulloides which occurs on Termination I. This acme can be correlated in cores near the upwelling zone (dashed line in Figure 6) and is best observed near the coast (MD77-203). The abundance peak decreases in magnitude offshore over several hundred miles and does not occur in the eastern or central Arabian Sea. The age of the abundance peak datum is about 9000 years on the basis of ^{14}C-dated $\delta^{18}O$ stratigraphy (Duplessy et al., 1981; Prell et al., 1980) and limited ^{14}C dates of V34-88.

A third major pattern is the low relative abundance of G. bulloides at the base of Termination I (correlated by the solid line in Figure 6). At this time, all cores proximal to the upwelling have about 20% G. bulloides with no apparent gradient within the proximal cores. The age of this minimum in G. bulloides abundance is estimated to be <18,000 YBP. Hence, G. bulloides was less abundant at the last glacial maximum (18,000 YBP) and, by inference, monsoonal upwelling was weaker (Prell et al., 1980). Alternatively, G. bulloides was more abundant and monsoonal upwelling more intense during the glacial-interglacial transition. Here, I note that the abundance peak is not coincident with so-called hypsithermal (approximately 6,000 YBP) but clearly falls on the transition between glacial and interglacial modes. Examination of cores from the central Arabian Sea (Figure 6) reveals only small variations in the abundance of G. bulloides. Hence, monsoonal upwelling variations are restricted to the western Arabian Sea, as expected for a coastal upwelling system.

These data provide us with a rough time series of how monsoonal upwelling has varied over the past 30,000 years. Of particular interest is the inference of weaker than present monsoonal upwelling during the last glacial maximum and stronger than present monsoonal upwelling during the glacial-interglacial transition. Next, I examine what climatic mechanisms or processes may have changed to account for the observed variation in monsoonal upwelling.

Past Monsoons

The geologic data reveal that the Southwest Monsoonal upwelling has been both weaker and stronger. The interpretation of these geologic data lead us to ask what boundary conditions have changed. Among the boundary conditions previously discussed, the seasonal distribution of solar radiation and the surface albedo are the most likely to have shown major changes over this time interval.

The albedo of the Asian continent definitely changes on both seasonal and long time scales (10^3 years). The most obvious albedo changes are due to the spatial extent and persistence of seasonal snow cover, which is likely linked to solar radiation patterns. Albedo changes are also caused by the succession of vegetational patterns as the region passes from glacial to interglacial climates (CLIMAP, 1976, 1981).

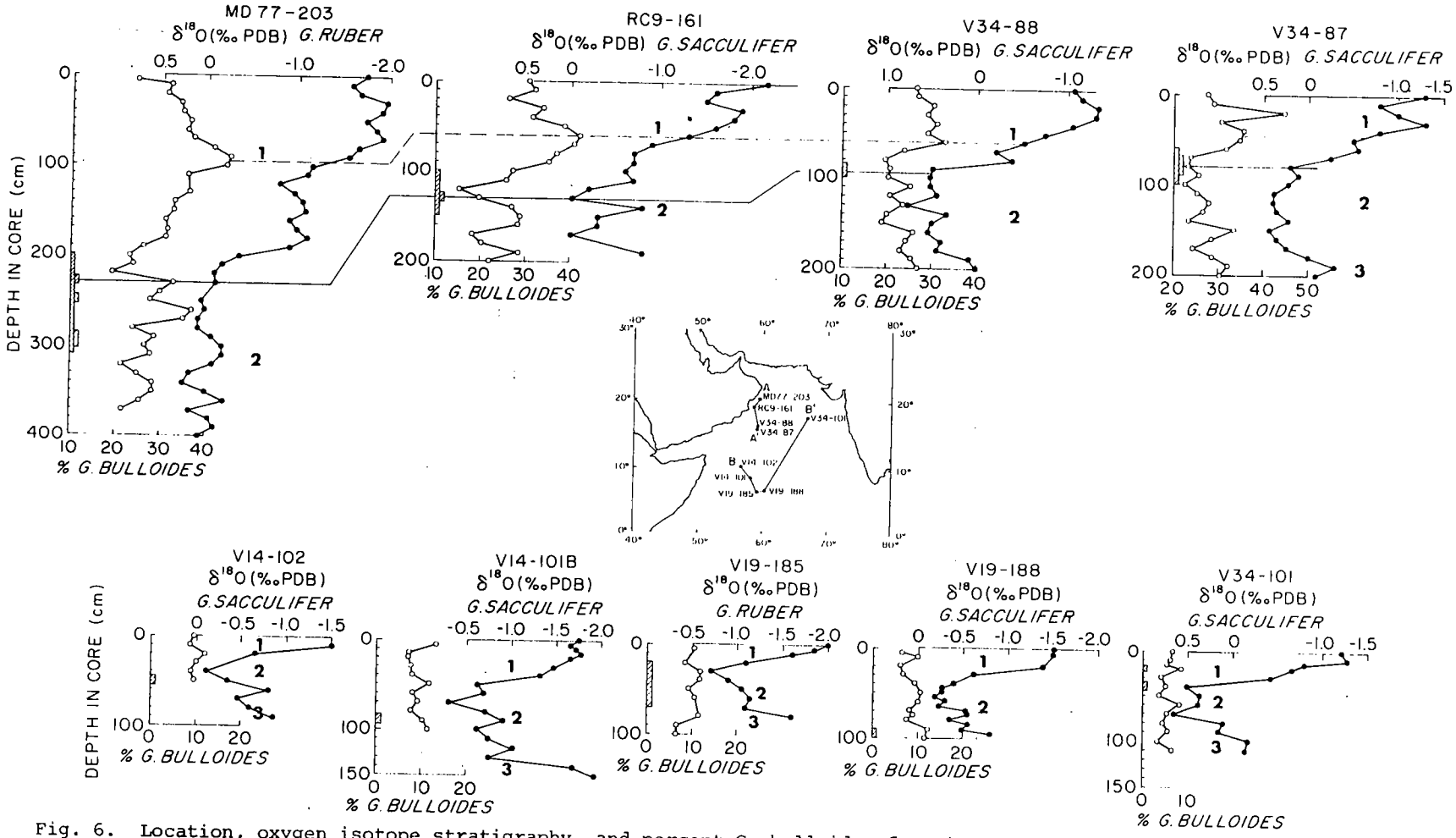

Fig. 6. Location, oxygen isotope stratigraphy, and percent G. bulloides for nine Arabian Sea cores. Isotope stages 1, 2 and 3 are shown in each core. Transect A-A' is proximal to coastal upwelling off Arabia, whereas transect B-B' is distal to the upwelling. The dashed line in transect A-A' correlates the G. bulloides maxima and the solid line correlates the G. bulloides minima and a brief occurrence of Globorotalia truncatulinoides (shown by bars on the depth axis). Isotopic data are from Prell et al., 1980; J. C. Duplessy (MD77-203) and this paper. Open circles denote the abundance of G. bulloides, and filled circles the oxygen isotope data.

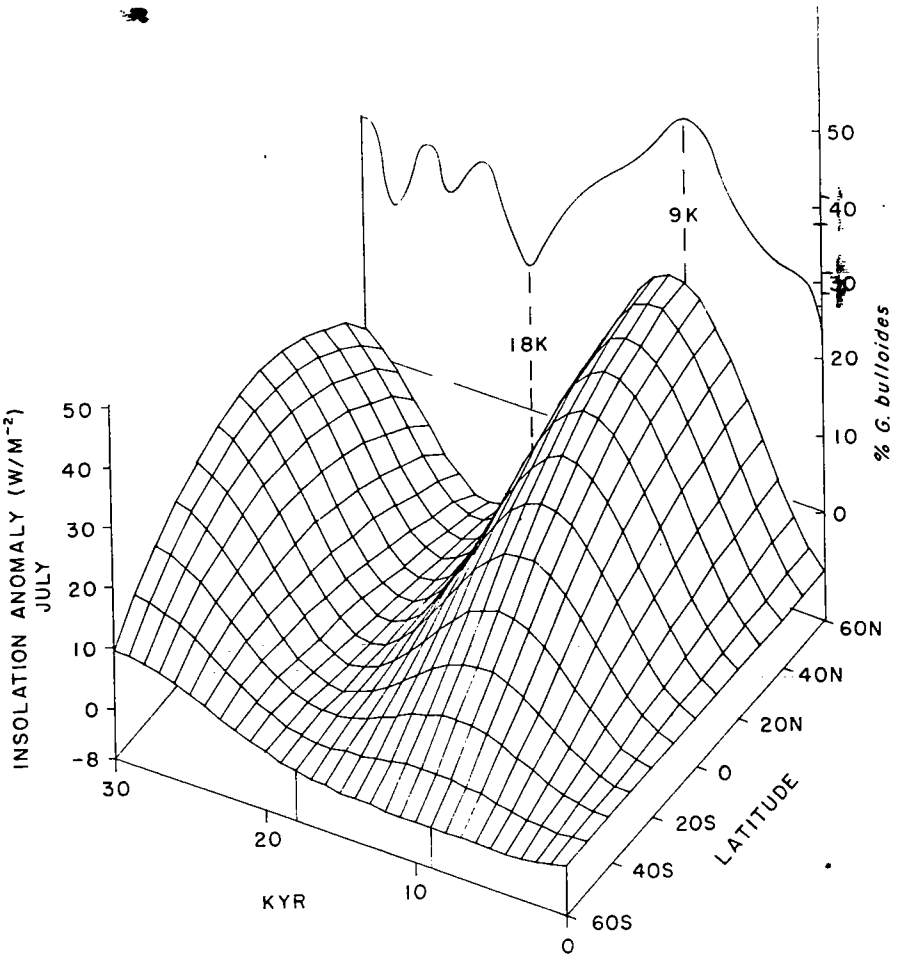

Fig. 7. Variation of solar insulation anomaly for July (past insulation-modern insulation, W/M^2) as a function of time (KYR=10^3yr) and latitude. Insulation values are calculated from Berger, 1979. A generalized curve of relative percent of G. bulloides, the upwelling index, is also shown on the same time scale.

Unfortunately, these vegetation and snow-cover patterns, and hence the resultant albedo, are difficult to quantify and map for past intervals. However, major changes in the distribution of Himalayan glaciers (Ahmad and Mayewski, in press) and vegetation patterns suggest that significant changes in albedo have occurred over Asia during the past 30,000 years.

The seasonal distribution of solar radiation has also exhibited significant changes over the past 30,000 years. The pattern of change is related to the shape of the Earth's orbit around the sun and has been calculated by numerous astronomers (for example, Milankovitch, 1941; Vernekar, 1972; and Berger, 1979). As an illustration of how solar radiation has changed with time and latitude, an insolation anomaly (past insolation - modern insolation) for July was calculated over the past 30,000 years for latitudes from 60°S to 60°N (Figure 7). This time-space diagram of the July insolation anomaly was selected because summer insolation should be the dominant driving force of the Southwest Monsoon. This diagram reveals several important features:

1. A maximum insolation anomaly occurs in the Northern Hemisphere at approximately 11,000 years B.P.
2. The insolation anomaly is minimal at 18,000 YBP and is quite similar to the modern distribution. Hence, during July the glacial maximum and modern solar radiation patterns are the same.
3. The insolation anomalies are strongly related to latitude.
4. The anomaly patterns for winter, not shown here, are essentially the reverse of the summer patterns. Hence, the annual anomaly is approximately zero.

These data show that the pattern of solar insolation during July undergoes major variations, which are latitude-dependent, over the past 30,000 years. Note also that the pattern of G. bulloides variation (Figure 7),

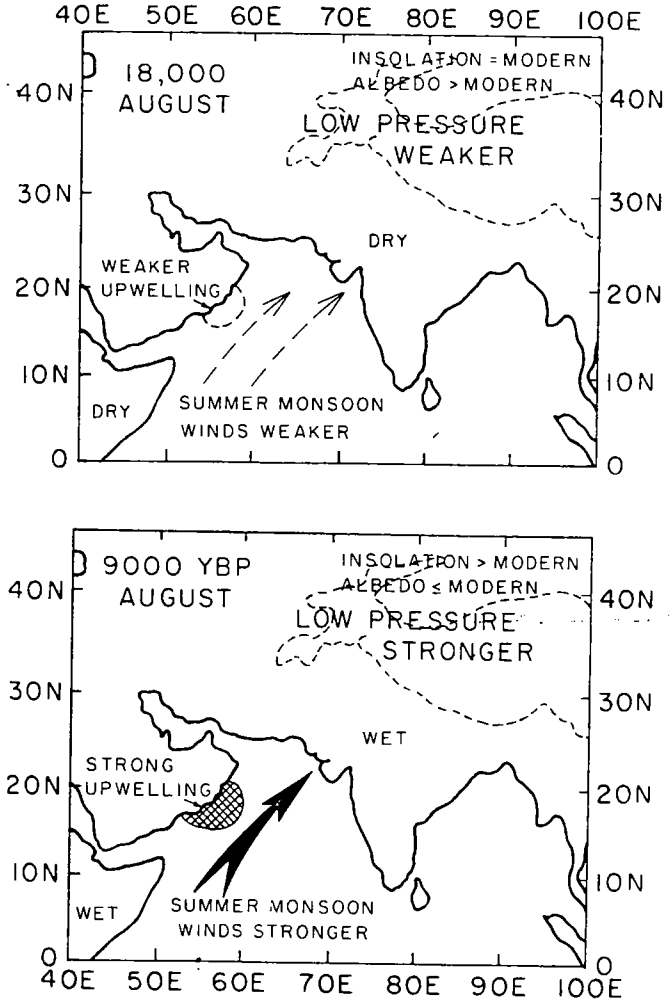

Fig. 8. Top: The inferred boundary conditions and circulation of the summer monsoon during the last glacial maximum (18,000 YBP) summer monsoon. Dashed arrows indicate weak monsoonal winds. Bottom: The inferred boundary conditions and circulation for the summer monsoon at 9000 YBP (the deglacial monsoon). The bold arrow indicates stronger monsoonal sinds and the checked area off Arabia indicates stronger than modern upwelling.

the index to monsoonal upwelling, is similar to that of the solar insolation anomaly pattern in the Northern Hemisphere.

The Glacial Maximum Monsoon (18,000 YBP)

Examination of the geologic and insolation data for the last glacial maximum about 18,000 years ago reveals that the insolation anomaly for July was about the same as today's but that monsoonal upwelling was weaker (Figure 7). Albedo was higher (CLIMAP, 1976, 1981). These observations suggest that the higher albedo led to less effective heating of the Tibetan Plateau and Asian continent and therefore the resultant summer low-pressure cell was weaker than in the modern climate. This weaker low-pressure cell over Asia created a lower pressure gradient from the central Indian Ocean to the Asian continent and hence less intense low-level monsoonal winds. Thus, the weak upwelling off Arabia is interpreted to reflect this decreased monsoonal intensity (Figure 8a). The weaker monsoonal upwelling is consistent with low lake levels throughout the region (Street and Grove, 1979) and enhanced precipitation in the equatorial zone (Duplessy, 1982). This interpretation is also consistent with GCM simulations of the last glacial maximum (Gates, 1976; Manabe and Hahn, 1977), which indicate a weaker monsoonal circulation.

The Deglacial Monsoon (9000 YBP)

Examination of the geologic and insolation data at 9000 YBP reveals that the amount of solar radiation is greater during the northern latitude summers and monsoonal upwelling is stronger (Figure 7). Note, however, that the maximum of upwelling does not exactly coincide with the maximum solar radiation in the Northern Hemisphere. Albedo is thought to be about the same as modern values. These observations, along with the results of Kutzbach (1981) and Kutzbach and Otto-Bliesner (1982), suggest that the higher summer insolation increased the heating of the Tibetan Plateau and Asian continent resulting in a stronger low-pressure cell. This enhanced low-pressure cell increases the pressure gradient between the Indian Ocean and the continental mass and hence causes the stronger monsoonal winds and increased upwelling (Figure 8b). The observation of increased upwelling is consistent with high lake levels in the surrounding areas (Street and Grove, 1979) and the transport of pollen off Africa into the Arabian Sea by southwesterly winds (van Campo et al., 1982).

Summary

In the modern climate, the Southwest Indian Monsoonal winds cause distinct areas of coastal upwelling along Arabia. This coastal upwelling is characterized by low sea-surface temperatures and high concentrations of nutrients. These upwelling conditions support distinct planktic faunal assemblages which are preserved in deep-sea sediments to record past variations in the monsoonal upwelling. Examination of this geologic record reveals that, compared to modern conditions, the Southwest Monsoonal upwelling has been both stronger and weaker during the past 30,000 years. This clear mechanistic linkage of the geologic record to the strength of monsoonal winds allows one to interpret the intensity of the Southwest Monsoon and to infer the boundary conditions which are consistent with the geologic record.

examination of the large-scale boundary conditions which control the intensity of monsoonal circulation suggest that changes in the distribution of seasonal solar radiation and surface albedo are responsible for the changes in the monsoon intensity. Changes in solar radiation, possibly modified by albedo feedbacks, are translated into climate change through their effect on the heating of the Asian continent and the creation of the pressure gradient between Asia and the Indian Ocean. Since the distribution of solar radiation is controlled by the variations of the Earth's orbit, the changing intensity of the Southwest Monsoon illustrates how small orbital variations may be translated into significant climate changes. These data suggest that the Milankovitch hypothesis applies to low-latitude climates, especially the monsoonal circulation, as well as high-latitude climate changes.

Acknowledgments. This research was supported by the Division of Atmospheric Sciences, National Science Foundation under grant ATM82-13296 to Brown University (W. L. Prell).

References

Ahmad, N., and Paul A. Mayewski, ____, Himalayan glaciation: an unresolved issue. (ms.)

Berger, A. L., 1979, Insolation signatures of Quaternary climatic changes: Il Nuovo Cimento, v. 2C, no. 1, p. 63-87.

CLIMAP Project Members, 1981, Seasonal reconstructions of the earth's surface at the last glacial maximum: Geol. Soc. Amer. Map and Chart MC-36.

CLIMAP Project Members, 1976, The surface of the ice-age Earth: Science, v. 191, p. 1131-1137.

Cullen, James L., 1980, Microfossil evidence for changing salinity patterns in the Bay of Bengal over the last 20 000 years: Palaeogeogr., Palaeoclimatol., Palaeoecol., v. 35: p. 315-356.

Duing, Walter, and Ants Leetma, 1980, Arabian Sea cooling: a preliminary heat budget: J. Phys. Oceanog., v. 10, no. 2, p. 307-312.

Duplessy, J.-C., G. Delibrias, J. L. Turon, C. Pujol, and J. Duprat, 1981, Deglacial warming of the northeastern Atlantic Ocean: correlation with the paleoclimatic evolution of the European continent: Palaeogeogr., Palaeoclimatol., Palaeoecol., v. 35, p. 121-144.

Duplessy, J.-C., 1982, Glacial to interglacial contrasts in the northern Indian Ocean revealed by oxygen isotopes: Nature, v. 295, p. 494-498.

Ganssen, Gerald, and Sarnthein, Michael, 1983, Stable-isotope composition of foraminifers: The surface and bottom water record of coastal upwelling: E. Suess and J. Thiede (eds.): Coastal Upwelling: Its Sediment Record

Gates, L. W., 1976, The numerical simulation of ice-age climate with a global general circulation model: J. Atmospheric Sci., v. 33, p. 184-1873.

Hahn, Douglas G., and Syukuro Manabe, 1975, The role of mountains in the south Asian monsoon circulation: J. Atmospheric Sci., v. 32, no. 8, p. 1515-1541.

Hastenrath, Stefan, and Peter J. Lamb, 1979, Climatic Atlas of the Indian Ocean: Univ. of Wisconsin Press, Madison, 97 charts, 19 p.

Hutson, William H., and Prell, Warren L., 1980, A paleoecological transfer function, FI-2, for Indian Ocean planktonic foraminifera: J. Paleon., v. 54, no. 2, p. 381-399.

Joint Scientific Committee for World Climate Research Programme and Global Atmospheric Research Programme, 1981, International Conference on the Scientific Results of the Monsoon Experiment: International Council of Scientific Unions, World Meteorological Organization Information Note No. 4, 164 p.

Krey, J., and B. Babenerd, 1976, Phytoplankton Production: Atlas of the International Indian Ocean Expedition: Intergovernmental Oceanographic Commission, UNESCO, 70 p.

Kutzbach, J. E., and B. L. Otto-Bliesner, 1982, The sensitivity of the African-Asian monsoonal climate to orbital parameter changes for 9000 years B.P. in a low-resolution general climate model: J. Atmospheric Sci., v. 39, no. 6, p. 1177-1188.

Kutzbach, J., 1981, Monsoon climate of the early Holocene: climate experiment using the Earth's orbital parameters for 9,000 years ago: Science, v. 214, p. 59-61.

Manabe, S., and D. G. Hahn, 1977, Simulation of the tropical climate of an Ice Age: J. Geophys. Res., v. 82, p. 3889-3911.

Milankovitch, M. M., 1941, Canon of Insolation and the Ice-Age Problem: Beograd, Koninglich Serbische Akademie. English translation by the Israel Program for Scientific Translation and published for the U. S. Department of Commerce and the National Science Foundation, Washington, D. C., 484 p.

Miller, Forrest R., and R. N. Keshavamurthy, 1968, Structure of an Arabian Sea Summer Monsoon System: Internat. Indian Ocean Expedition Meteor. Monogr. No. 1, East-West Center Press, Honolulu, 9 p.

Prell, Warren L., and Harold F. Streeter, 1982, Temporal and spatial patterns of monsoonal upwelling along Arabia: a modern analogue for the interpretation of Quaternary SST anomalies: J. Mar. Research, v. 40, no. 1, p. 143-155.

Prell, W. L., W. H. Hutson, D. F. Williams, A. W. H. Be, K. Geitzenauer, and B. Molfino, 1980, Surface circulation of the Indian Ocean during the last glacial maximum, approximately 18,000 yr B.P.: Quat. Res., v. 14, p. 309-336.

Ramage, C. S., 1971, Monsoon Meteorology: Internat. Geophys. Series No. 15, Academic Press, New York, 296 p.

Fred, and Bolli, Hans M., 1973, Holocene
Pleistocene planktonic foraminifera of Leg
, Site 147 (Cariaco Basin, Caribbean Sea)
d their climatic interpretation: Initial
eports of the Deep Sea Drilling Project, v.
V, p. 553-615.
eet, F. Alayne, and A. T. Grove, 1979, Global
aps of lake-level fluctuations since 30,000
yr B.P.: Quat. Res., v. 12, p. 83-118.
n Campo, E., J.-C. Duplessy, and M.
Rossignol-Strick, 1982, Climatic conditions
deduced from a 150-kyr oxygen isotope-pollen
record from the Arabian Sea: Nature, v. 296,
p. 56-59.
Vernekar, A. D., 1972, Long-Period Global
Variations of Incoming Radiation: Meteorol.
Monogr. No. 34, Amer. Meteor. Soc., 21 p.
Wyrtki, Klaus, 1971, Oceanographic Atlas of the
International Ocean Expedition: National
Science Foundation, Washington, D. C., 531 p.